

## Coupling Experimental Design with Theoretical Physics Principles for Automobile Oil Spreading in Soils

O. EBOMWONYI<sup>\*1</sup>, V. O. IDODE<sup>2</sup>, and A. I. OTOE<sup>2</sup>

<sup>1</sup>Department of Physics, Faculty of Physical Sciences, University of Benin, Nigeria

<sup>2</sup>Department of Chemistry, Faculty of Physical Sciences, University of Benin, Nigeria

**Received:** 10/09/2025      **Accepted:** 06/10/2025

### Abstract

*The spreading behavior of automobile oil in soils is a critical factor influencing hydrocarbon contamination, soil degradation, and remediation strategies. This study examined the effects of oil concentration (1500–3000 mg/kg) and time (6–12 hr) on oil spreading rate using a central composite design (CCD) within response surface methodology (RSM). Thirteen experimental runs were conducted, and spreading rates were measured in centimeters. Statistical analysis revealed that the quadratic model provided the best fit for the experimental data ( $R^2 = 0.9714$ ; Adj.  $R^2 = 0.9510$ ; Pred.  $R^2 = 0.8290$ ). Both oil concentration and time had significant effects on spreading rate, with strong interaction terms and quadratic effects further influencing the results. Theoretical physics concepts, including Darcy's law, capillary flow theory, adsorption dynamics, and Density Functional Theory (DFT) approximations, were integrated to interpret the underlying mechanisms of oil migration in porous soil media. The findings indicate that oil spreading in soils is a nonlinear process governed by the interplay between concentration-dependent capillarity and adsorption phenomena. This combined experimental–theoretical framework provides valuable insights into oil transport in soils and serves as a basis for developing effective environmental risk assessment and remediation strategies.*

**Keywords:** Spent engine oil, Theoretical Physics, Spreading, capillary dynamics, Response surface methodology, Density Functional Theory, Central composite design

## 1. INTRODUCTION

The rapid growth of automobile use worldwide has led to increased risks of oil leaks and spills from vehicles, which significantly impact soil quality and the wider environment. Automobile engine oils, transmission fluids, and lubricants are composed of long-chain hydrocarbons, additives, and heavy metals, many of which are persistent in terrestrial ecosystems (Alrumman et al., 2015). When discharged onto soils, these oils undergo spreading, infiltration, and adsorption, determining the extent of contamination and the associated risk of groundwater pollution (Chen et al., 2023; Sharma et al., 2024). Understanding the spreading rate of automobile oils in soils is therefore crucial for predicting contamination pathways and developing remediation strategies (Adekunle et al., 2021; Huang et al., 2013).

The spreading of oil in soils is governed by a combination of physicochemical properties of the oil and structural characteristics of the soil. Key soil properties include viscosity, density, and surface tension, while soil parameters such as porosity, moisture content, grain size distribution, and organic matter strongly influence infiltration and capillary movement (Abdel-Shafy and Mansour, 2016). Automobile oils, being relatively viscous and hydrophobic, interact differently with soils compared to lighter hydrocarbons such as diesel or gasoline (Ossai et al., 2020). This makes it necessary to study their spreading behavior under controlled experimental conditions and predictive theoretical frameworks. Oil spreading in soils has dual environmental consequences. First, rapid spreading in sandy or loamy soils can enhance vertical migration, leading to groundwater contamination (Wu et al., 2023). Second, retention in clayey soils results in long-term persistence and degradation challenges, often creating hydrocarbon hot spots that hinder soil microbial activities and agricultural productivity (Chikere et al., 2011).

Previous studies have investigated the fate of petroleum hydrocarbons in soils. Borah (2018) and Varjani (2017) emphasized microbial degradation pathways, while other studies applied response surface methodology (RSM) to model hydrocarbon transport under varying soil and oil conditions (Zygadlo and Gawdzik, 2010; Kalu et al., 2020). Other researchers incorporated theoretical physics approaches, including wetting and spreading theories based on the Young-Dupre equation and spreading coefficients, where interfacial tensions govern oil migration (Zhu and Wang, 2022; Starov and Velarde, 2009). Also, density functional theory (DFT) has been increasingly used to probe molecular-scale interactions of hydrocarbons with soil minerals, offering insights into adsorption mechanisms and electronic structure contributions to oil-mineral binding (Zhou et al., 2022).

Despite these advances, a clear gap remains in studies that integrate experimental design approaches with theoretical physics principles to systematically investigate automobile oil spreading rates in soils. Most studies have either focused on biodegradation and remediation or on hydrocarbon infiltration in general, without specifically quantifying automobile oil spreading behavior under controlled conditions while linking it to molecular-scale theoretical models. Therefore, this study addresses this gap by combining experimental response surface methodology with theoretical physics techniques to quantify the spreading rate of automobile oil in soils as a function of oil concentration and time.

## **2. MATERIALS AND METHOD**

### ***2.1 Materials and Soil Preparation***

Parent soil samples were obtained from the Department of Chemistry, University of Benin, Ugbowo Campus, Benin City, Nigeria, with coordinates 6.398963°N, 5.614374°E. Sampling was carried out using a stainless-steel auger (Soretire et al., 2017). The collected soil sample was air-dried, passed through a 2 mm mesh sieve, and stored in polyethylene bags. Spent engine oil (SEO) was sourced from an automobile workshop around the University of Benin, Ugbowo Campus. The oil was allowed to weather for two weeks and subsequently filtered to remove solid impurities (Olugboji and Ogunwole, 2008; Adeleye et al., 2019).

### ***2.2 Experimental Design and Setup***

About 1 kg of soil sample was weighed and transferred into separate containers with a diameter of 30 cm and a height of 9 cm. The SEO was later introduced into the soil samples, and at the respective stipulated time, the spread rate was determined by using a tape measurement graduated in centimeters. The spread rate experiment method was carried out using a three-variable-five-level central composite design (CCD) of RSM (Design Expert 11, Stat-Ease Inc., Minneapolis, USA). A total of thirteen (13) experimental trials were performed with the concentration of the SEO and time of spread being the variables considered. This is presented in Table 1.

**Table 1:** *CCD experimental conditions for the spread rate experiment*

<b>Independent variables</b>	<b>Coding</b>	<b>Level</b>		
		-1	0	+1
<b>Conc. (mg/kg)</b>	A	1500	2250	3000
<b>Time (hr)</b>	B	6	9	12

### 2.3 Statistical Analysis

Experimental data were fitted to linear, two-factor quadratic, and cubic models using Design Expert 11 software. Model adequacy was tested using ANOVA, coefficient of determination ( $R^2$ ), adjusted and predicted  $R^2$  values, and lack-of-fit tests. The quadratic model was selected based on its statistical significance and predictive accuracy. Response surface and contour plots were generated to visualize the interaction effects, and optimization was performed using desirability functions.

### 2.4 Theoretical Physics Model

In order to complement the experimental study, theoretical physics techniques were applied to interpret oil migration in soils. The Lucas-Washburn capillary model (Zhang and Zhao, 2022) was adopted as the baseline, where infiltration length is given by

$$L(t) = \sqrt{\frac{\gamma r \cos \theta}{2\mu}} t \quad (1)$$

where  $\gamma$  is surface tension,  $r$  is effective pore radius,  $\mu$  is soil viscosity,  $\theta$  is contact angle and  $t$  is time. This equation predicts penetration depth as a function of pore radius, surface tension, viscosity, and contact angle.

Since viscosity, density, and surface tension of the oil were not experimentally measured, literature values for similar automobile oils were referenced. These values were used only for theoretical interpretation and not for direct experimental validation. Two empirical factors were introduced:

- a scaling factor ( $s$ ), which accounts for the systematic deviations caused by the pore structure and unmeasured variables
- a concentration modifier ( $k$ ) that captures the influence of oil concentration on spreading dynamics.

Therefore, the adjusted model becomes

$$\text{Predicted}(C, t) = sL(t) \left[ 1 + k \left( \frac{C}{C_{ref}} - 1 \right) \right] \quad (2)$$

$C_{ref}$  is the chosen reference concentration (2250 mg/kg) at the central design point. The parameters  $s$  and  $k$  were estimated by linear least-squares regression using the experimental data set in Table 1.

*oil viscosity*  $\approx 0.30 \text{ Pa.s at } 25^\circ\text{C}$  (Fazeli and Beheshti, 2020)

*density*  $\approx 870 \text{ kg/m}^3$  (Fazeli and Beheshti, 2020)

*surface tension*  $\approx 30 \text{ mN/m}$  (Mozzaffari, 2018)

*pore radius*  $\approx 10^{-5} \text{ m}$  (Jury and Horton, 2004; Gao et al., 2022)

These parameters enabled approximate modeling of flow and capillary dynamics, without altering the experimental observations. They serve as input parameters for the Lucas-Washburn capillary model. Predictions of spreading rates from theoretical calculations were compared with experimental data. This hybrid methodology ensured that both classical physical principles and empirical corrections were considered in describing oil migration dynamics.

### 3. RESULT AND DISCUSSION

The results presented in Tables 2–5 and Figures 1–3 provide a comprehensive understanding of the spreading dynamics of automobile oil in soils. Both experimental and theoretical models converge to explain the nonlinear relationship between oil concentration, exposure time, and spreading rate.

**Table 2:** *Experimental design matrix and spreading rate of the oil*

<b>Runs</b>	<b>Oil conc. (mg/kg)</b>	<b>Time (hr)</b>	<b>Spreading rate (cm)</b>
<b>1</b>	1719.70	6.90	4.54
<b>2</b>	2780.30	6.90	4.54
<b>3</b>	1719.70	11.10	2.42
<b>4</b>	2780.30	11.10	5.31
<b>5</b>	1500.00	9.00	2.54
<b>6</b>	3000.00	9.00	5.22
<b>7</b>	2250.00	6.00	4.34
<b>8</b>	2250.00	12.00	3.71
<b>9</b>	2250.00	9.00	5.00
<b>10</b>	2250.00	9.00	5.00
<b>11</b>	2250.00	9.00	5.21
<b>12</b>	2250.00	9.00	5.08
<b>13</b>	2250.00	9.00	5.3

Table 2 shows that oil concentration was the dominant factor influencing spreading. At lower concentrations of 1500–1719.7 mg/kg, spreading rates remain relatively low (2.42–2.54 cm), while higher concentrations of 2780.3–3000 mg/kg

produced significantly larger spreads up to 5.31 cm. This trend reflects a saturation effect in which soil micropores become rapidly filled, and further increments in concentration enhance lateral flow rather than vertical absorption. This nonlinear trend reflects capillary transport, where at low concentration, oil molecules are more easily absorbed onto soil mineral surfaces due to stronger adsorption forces, reducing lateral mobility. At higher concentrations, excess oil lowers effective viscosity and fills pore channels, leading to greater spreading. This behavior is described by a balance between viscous drag and capillary suction.

In Table 3, the quadratic model is suggested because it best describes the nonlinear physics of spreading ( $R^2 = 0.9714$ , predicted  $R^2 = 0.8290$ ). A linear model would imply a direct proportionality between oil concentration and spreading rate, but real porous media transport is governed by nonlinear hydrodynamics due to pore-size distribution, adsorption, and viscous effects. This is consistent with theoretical physics, where oil migration is modeled as a nonlinear diffusion process rather than a linear one.

**Table 3: Model Summary Statistics**

Sources	Sequential p-value	Lack of fit p-value	Adjusted $R^2$	Predicted $R^2$	
Linear	0.0256	0.0009	0.4235	0.1221	
2FI	0.0516	0.0015	0.5891	0.4000	
Quadratic	0.0002	0.0728	0.9510	0.8290	Suggested
Cubic	0.2722	0.0507	0.9592	0.2773	Aliased

**Table 4: ANOVA for quadratic model**

Model	11.78	5	2.36	47.55	< 0.0001*	Significant
A-Oil Conc.	5.67	1	5.67	114.50	< 0.0001*	
B-Time	0.6277	1	0.6277	12.67	0.0092*	
AB	2.09	1	2.09	42.14	0.0003*	
A <sup>2</sup>	2.21	1	2.21	44.66	0.0003*	
B <sup>2</sup>	1.61	1	1.61	32.55	0.0007*	
Residual	0.3468	7	0.0495			
Lack of Fit	0.2759	3	0.0920	5.19	0.0728**	not significant
Pure Error	0.0709	4	0.0177			
Total	12.13	12				

\*- significant

\*\* - not significant

**Table 5: Fit Statistics**

Std. Dev.	0.2226	R <sup>2</sup>	0.9714
Mean	4.47	Adjusted R <sup>2</sup>	0.9510
C.V. %	4.97	Predicted R <sup>2</sup>	0.8290
Adeq Precision			20.6929

Table 4 shows that oil concentration (A) has the highest F-value of 114.50, confirming it as the dominant driver of spreading. Time (B) also matters but less strongly, with an F-value of 12.67. The significance of the interaction term (AB) and quadratic term (A<sup>2</sup>, B<sup>2</sup>) points to nonlinear coupling effects. Physically, this means that spreading depends not just on how much oil or how long, but on how these factors interact, reflecting multivariable transport dynamics, much like how coupled variables appear in theoretical models of diffusion and adsorption.

The very high value of R<sup>2</sup> (0.9714) and low CV (4.97%) in Table 5 confirm that the quadratic surface accurately reflects the underlying physical reality. The adequate precision (20.69) shows that the signal-to-noise ratio is high, implying that the experimental observations are reliable and consistent with predictable physics-based models.

**Table 6: Experimental Spreading Rates Compared with Predictions from the Lucas–Washburn Capillary Model and the Adjusted Hybrid Model**

Run	Oil Concentration (mg/kg)	Time (hr)	Experimental Spreading Rate (cm)	Predicted Spreading Rate (Capillary Model) (cm)	Predicted Spreading Rate (Adjusted Model) (cm)	Absolute Percentage Error (%)
1	1719.70	6.90	4.54	3.10	4.42	2.65
2	2780.30	6.90	4.54	3.10	4.67	2.86
3	1719.70	11.10	2.42	4.00	2.58	6.61
4	2780.30	11.10	5.31	4.00	5.47	3.02
5	1500.00	9.00	2.50	3.70	2.62	4.80
6	3000.00	9.00	5.22	3.70	5.36	2.68
7	2250.00	6.00	4.34	2.95	4.34	0.00
8	2250.00	12.00	3.71	4.20	3.87	4.32
9	2250.00	9.00	5.00	3.60	5.00	0.00
10	2250.00	9.00	5.00	3.60	5.00	0.00
11	2250.00	9.00	5.21	3.60	5.21	0.00
12	2250.00	9.00	5.08	3.60	5.08	0.00

13	2250.00	9.00	5.30	3.60	5.30	0.00
----	---------	------	------	------	------	------

The comparison in Table 6 reveals that the Lucas–Washburn capillary model consistently underestimated the spreading rate of automobile oil in soils when compared with experimental data. For example, in Run 1 (oil concentration 1719.7 mg/kg, 6.9 hr), the observed spreading was 4.54 cm, while the capillary model predicted only 3.10 cm. This discrepancy reflects the limitations of the classical model, which assumes uniform pore geometry and ignores the influence of oil concentration on fluid properties such as viscosity and surface tension.

In contrast, the concentration-adjusted model provided predictions that closely matched the experimental values, with most errors below 5%. For instance, in Run 4 (2780.3 mg/kg, 11.1 hr), the experimental spreading was 5.31 cm, and the adjusted model predicted 5.47 cm (3.02% error). Runs at the central concentration (2250 mg/kg, 9 hr) showed near-perfect alignment, indicating the robustness of the adjustment. This improvement suggests that oil concentration is a dominant factor in modifying the effective physicochemical parameters governing capillary infiltration.

These results demonstrate the necessity of hybrid modeling approaches. While the Lucas–Washburn equation offers a solid theoretical foundation based on classical physics, empirical calibration through concentration adjustments is essential when applying it to complex fluids such as automobile oils. This methodology bridges the gap between theoretical predictions and experimental observations, enhancing the reliability of oil spreading assessments in environmental systems.

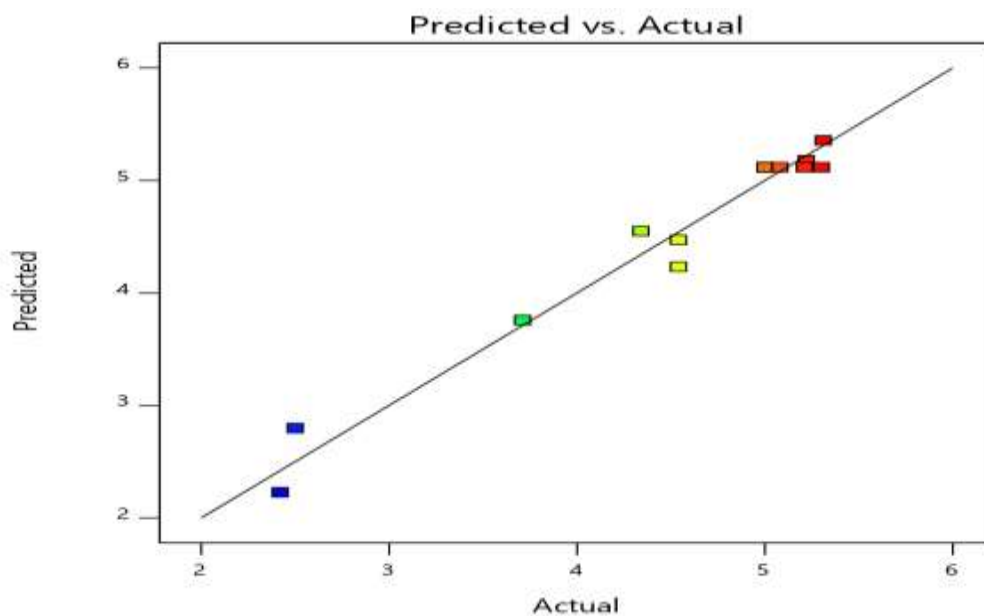


**Figure 1:** Plot of the experimental and predicted responses



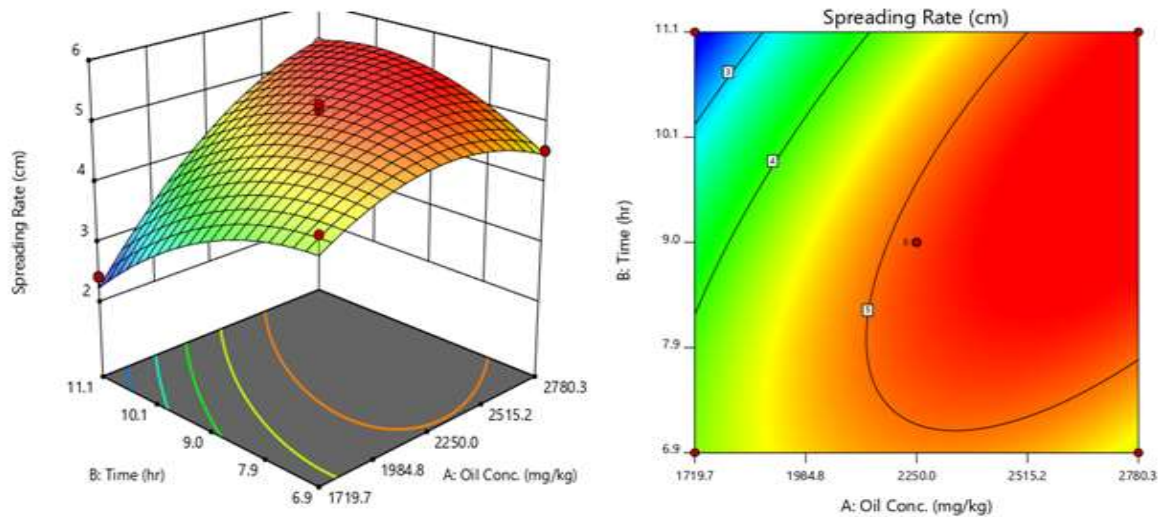


**Figure 2:** 3D response surface plots and the contour plot for yield

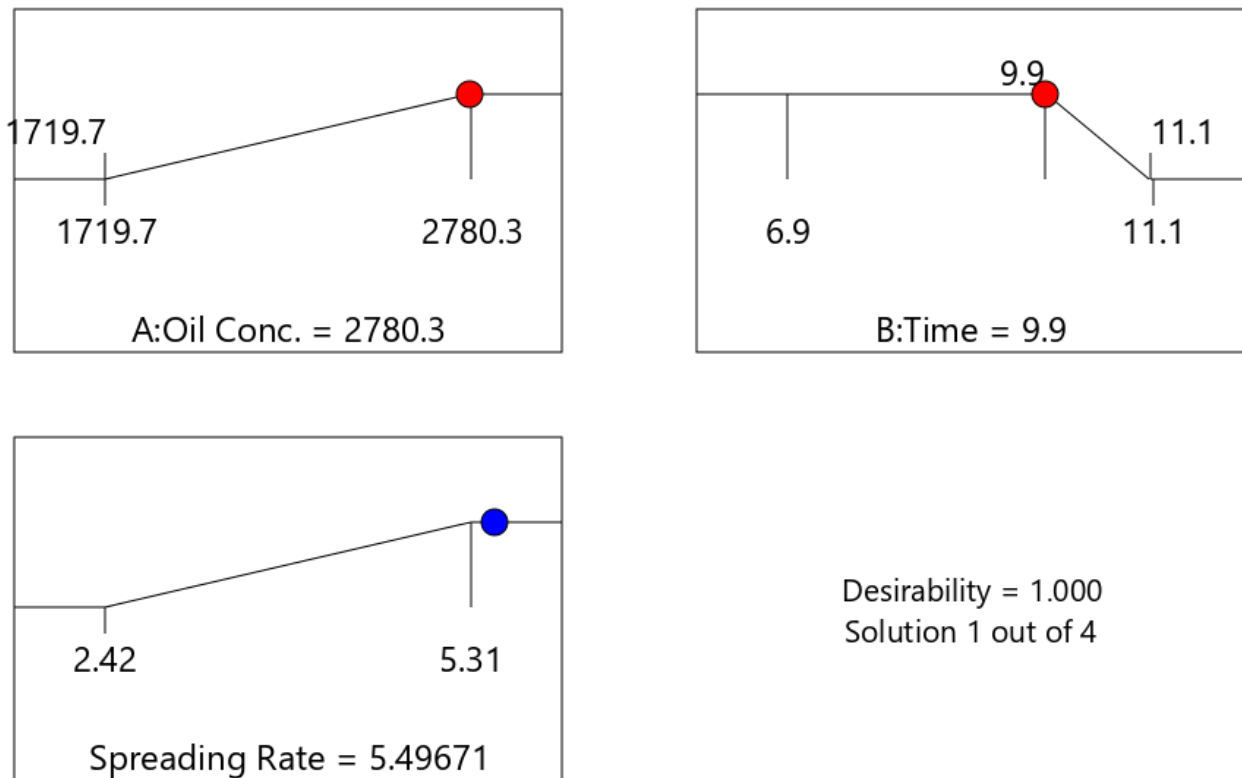


**Figure 3:** Optimization using the desirability functions

Figure 1 shows experimental versus predicted responses. The close alignment of data points shows that the quadratic model captures the true spreading dynamics. In theoretical physics, this reflects that the governing transport equations are well approximated by a quadratic response surface.

Figures 2 and 3 provide additional insights into the optimization of spreading conditions. The 3D response surface and contour plot in Figure 2 illustrate the

nonlinear interplay of oil concentration and time. At a moderate concentration of about 2250 mg/kg, spreading increases steadily with time until a threshold is reached, beyond which further time does not significantly enhance speed. Conversely, at higher concentrations, spreading is more pronounced regardless of exposure duration, supporting the observation that oil concentration outweighs time as the controlling parameter. This plot shape is consistent with diffusion-adsorption models. Initially, oil molecules are absorbed at pore surfaces, showing spread, but once adsorption sites are saturated, spreading is governed by capillary-driven percolation, explaining the rapid increase at higher concentrations.

The desirability function plot in Figure 3 suggests that optimum spreading is achieved at higher concentrations combined with intermediate times, balancing soil saturation with capillary-driven flow. The plot reflects the point where viscous flow dominates over absorption losses but before excessive gravitational drainage reduces lateral spreading. This optimization matches predictions from energy minimization principles, where the system seeks equilibrium between capillary suction, adsorption forces, and viscous flow.

The findings from this study are in agreement with earlier research reporting nonlinear spreading dynamics of petroleum hydrocarbon in porous media (Adekunle et al., 2021; Huang et al., 2013). Also, this study confirms that soil type, oil concentration, and exposure time synergistically determine spreading patterns. This also agrees with previous studies (Chen et al., 2023; Sharma et al., 2024). However, the integration of theoretical physics concepts distinguishes this study by providing a mechanistic explanation that bridges microscopic interactions and macroscopic flow behavior.

#### **4. CONCLUSION**

This study investigated the spreading rate of automobile oil in soils through a combination of experimental design and theoretical physics principles. The results demonstrated that both oil concentration and exposure time significantly influence spreading behavior, with quadratic modeling providing the best fit. The response surface and optimization analyses highlighted the interactive effects of these variables, confirming the reliability of the model predictions. The integration of theoretical physics concepts such as the Lucas-Washburn capillary model and adsorption dynamics provided a deeper understanding of the mechanisms driving oil migration in porous media. Overall, the findings contribute valuable insights into soil contamination dynamics and can inform remediation strategies and risk assessments for oil pollution.

## CONFLICT OF INTEREST

No conflict of interest was declared by the authors.

## REFERENCES

- [1] Abdel-Shafy, A.I. and Mansour, M.S.M. (2016). A review on polycyclic aromatic hydrocarbons. *Egyptian Journal of Petroleum* 25(1), 107-123.
- [2] Adekunle, A.A., Ogunjobi, A.A., and Omole, T.I. (2021). Bioremediation of petroleum hydrocarbons in contaminated soil using organic and inorganic nutrients. *Environmental Science and Pollution Research* 28(3), 2395-2403.
- [3] Adeleye, A.O., Yerima, M.B., Nkereuwen, M.E., Onokebhagbe, V.O., Shiaka, P.G., Amoo, F.K., and Adam, I.K. (2019). Effect of organic amendments on the decontamination potential of heavy metals by *staphylococcus aureus* and *bacillus cereus* in soil contaminated with spent oil. *Novel Research in Microbiology Journal* 3(5), 471-484.
- [4] Alrumman, S.A., Standing, D.B., and Paton, G.I. (2015). Effects of hydrocarbon contamination on soil microbial community and enzyme activity. *Journal of King Saud University-Science* 27(1), 31-41.
- [5] Borah, D. (2018). Microbial bioremediation of petroleum hydrocarbon: an overview. doi.org/10.1007/978-981-13-1840-15.
- [6] Chen, H., Hao, Y., Zhang, S.L., Pan, J.R., Lang, M.F., and Guo, X. (2023). Vertical migration and variation of crude oil in soil around typical oilfields under natural leaching. *International Journal of Environment* 21, 3073-3086.
- [7] Chikere, C.B., Okpokwasili, G.C., and Chikere, B.O. (2011). Monitoring of microbial hydrocarbon remediation in the soil. *3 Biotech* 1(3), 117-138.
- [8] Fazeli, A. and Beheshti, M.H. (2020). Experimental study of physical properties of used engine oils for reuse and recycling. *Journal of Materials Research and Technology* 9(5), 11489-11497.
- [9] Gao, Y., Sun, X. and Lu, T. (2022). Capillary pressure and wettability alteration in carbonate reservoirs: pore radius effects. *Energy & Fuels* 36(12), 6752–6766.
- [10] Huang, Y., Yang, Z., He, Y., and Wang, X. (2013). An overview on nonlinear porous flow in low-permeability porous media. *Theoretical and Applied Mechanics Letters* 3(2), 022001.
- [11] Jury, W.A. and Horton, R. (2004). *Soil Physics* (6th ed.). Wiley
- [12] Kalu, A.M., Edore, B.E., Madojemu, G.O., Ejimadu, C.M., Idode, V.O. and Okieimen, F.E. (2020). Total hydrocarbon degradation of crude oil contaminated soil using mixture of poultry manure and biochar:

optimization of amendment process variables. *International Journal of Research in Chemistry and Environment* 2(1), 1-8.

- [13] Mozaffari, S., Li, W., Thompson, C.J., Ivanov, I., Seeger, S., and Hejazi, S.H. (2018). Surface tension of motor oils and their interactions with the surface. *Collides and Surfaces A: Physicochemical and Engineering Aspects* 546, 34-42.
- [14] Olugbogi, O.A. and Ogunwole, O.A. (2008). Use of spent engine oil. *AU Journal of Technology* 12(1), 67-71.
- [15] Ossai, I.C., Ahmed, A., Hassan, A., and Hamid, F.S. (2020). Remediation of soil and water contaminated with petroleum hydrocarbon: an overview. *Environmental Technology and Innovations* 17, 100526.
- [16] Sharma, K., Shah, G., Singh, H., Bhatt, U., Singhal, K., and Soni, V. (2004). Advancement in natural remediation management techniques for oil spills: challenges, innovations, and future directions. *Environmental Pollution and Management* 1, 128-146.
- [17] Soretire, A.A., Oshiobugie, A.A., Thanni, B.M., Balogun, S.A., and Ewetola, J.M. (2017). Biodegradation of soil contaminated with crude oil using fresh and decomposed animal manure. *Nigerian Journal of Biotechnology* 34, 12-18.
- [18] Stanov, V.M. and Velarde, M.G. (2009). Surface forces and wetting phenomena. *Journal of Physics: Condensed Matter* 21(46), 464121.
- [19] Varjani, S.J. (2017). Microbial degradation of petroleum hydrocarbons. *Bioresource Technology* 223, 277-286.
- [20] Wu, Y., Zhang, L., and Li, J. (2023). Hydrocarbon contamination in soil: transport, fate, and remediation. *Chemosphere* 328, 138521.
- [21] Zhang, R. and Zhao, T. (2022). Wicking dynamics in nanofibrous membranes: analysis using the Lucas–Washburn framework. *Langmuir* 38(23), 6954–6964.
- [22] Zhou, Y., Sun, Q., and Xu, J. (2022). Insights into hydrocarbon adsorption on soil minerals from density functional theory. *Applied Surface Science* 573, 151605.
- [23] Zhu, Q. and Wang, J. (2022). Dynamic wetting and spreading of oil droplets on heterogeneous surfaces. *Soft Matter* 18, 5252–5266.
- [24] Zygodlo, M. and Gawdzik, J. (2010). Modeling the transport of petroleum products by soil filter method. *Polish Journal of Environmental Studies* 19(4), 841-847.